

UCSF

UC San Francisco Electronic Theses and Dissertations

Title

Decoding Pain Anticipation Imaging Biomarkers using fMRI BOLD Contrast in Patients with cLBP

Permalink

<https://escholarship.org/uc/item/9mn5987x>

Author

Zhang, Jiaxiuxiu

Publication Date

2022

Peer reviewed|Thesis/dissertation

Decoding Pain Anticipation Imaging Biomarkers using fMRI BOLD Contrast in Patients with cLBP

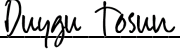
by
Jiaxiuxiu Zhang

THESIS
Submitted in partial satisfaction of the requirements for degree of
MASTER OF SCIENCE

in
Biomedical Imaging

in the
GRADUATE DIVISION
of the
UNIVERSITY OF CALIFORNIA, SAN FRANCISCO

Approved:

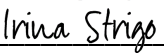
DocuSigned by:

A2C3822F2671486...
Duygu Tosun
Chair

DocuSigned by:

45D...
Fei Jiang

DocuSigned by:

42C...
Valentina Padoia

DocuSigned by:

858DE5F00147486...
Irina Strigo

Committee Members

Copyright 2022

by

Jiuxiu Zhang

Acknowledgements

First and foremost, I would like to thank Dr. Duygu Tosun-Turgut for serving as the chair of my committee and offering such steadfast support and guidance throughout this process. I would also like to thank Dr. Irina Strigo for helping me acquire data for this project and for sharing knowledge in pain perception and anticipation. Lastly, I would like to acknowledge the shared expertise and valuable feedback provided by Dr. Valentina Pedoia, Dr. Fei Jiang, and Dr. Pamela Zobel-Thropp.

Decoding Pain Anticipation Imaging Biomarkers using fMRI BOLD Contrast in Patients with cLBP

Jiaxiuxiu Zhang

Abstract

Pain is known to have sensory, cognitive, and affective aspects. However, the mechanism behind individual perception and anticipation of pain remains a question in the field. In this investigation, 26 subjects who suffered from varying levels of severity of chronic low back pain (cLBP) were recruited into a neuroimaging study which included structural magnetic resonance imaging (MRI) and evoked pain paradigm functional MRI (fMRI) experiments. During evoked pain paradigm fMRI experiments, participants received randomized cues on the intensity of the upcoming pain stimulations (either high, low, or uncertain). Their structural images were input into segmentation tools to measure the volume of 31 regions of interest (ROIs). fMRI images were collected, preprocessed, and then processed to build individual activation maps. Daily experience with cLBP was also collected through self-reporting PEG (Pain, Enjoyment, General activity) scores. We assessed to what extent brain structure volumes were associated with self-reported PEG scores. Further, we built logistic regression models with LASSO penalization for each subject separately to test three things: 1) if neural patterns of each cLBP patient were separable when perceiving high pain and low pain stimulus; 2) if high pain and low pain anticipation brain activation patterns of cLBP patients were distinguishable during known anticipation cues; and 3) if brain activation during known anticipation cue states could be used to decode each cLBP patient's anticipation bias during uncertain cue states. All analyses focused on structural and neuronal activation measures from a priori selected brain regions including subfields of insula, nucleus accumbens, substantia nigra, anterior cingulate cortex, amygdala, caudate nucleus, putamen, pallidum, subgenual frontal cortex, and thalamus. The linear regression models showed that the volumes of left insula middle short gyrus, right insula anterior inferior cortex and bilateral

anterior cingulate cortex were negatively associated with PEG scores, which reflect their daily experience with cLBP. The LASSO model built for individuals separating high pain and low pain perception had an average area under the curve (AUC) 0.773 ± 0.206 and the accuracy of prediction was 0.65 ± 0.179 . The LASSO model built for each individual separating high pain anticipation and low pain anticipation has an average AUC of 0.861 ± 0.218 and accuracy of prediction of 0.75 ± 0.21 . Furthermore, the linear regression models assessing the association of 1) regional activation during pain perception, 2) regional activation during pain anticipation, 3) individual anticipatory bias decoded for uncertain cue states with PEG scores were not statistically significant in this cLBP cohort. Thus, we were not able to explain individually perceived severity of cLBP by their neuronal activation and anticipatory bias, but their brain morphometry changes in this study.

Table of Contents

Introduction	1
Methods	3
Results	12
Discussion	22
References	25

List of Figures

Figure 1.....	5
Figure 2.....	8
Figure 3.....	12
Figure 4.....	13
Figure 5	14
Figure 6	15
Figure 7	17
Figure 8	17
Figure 9	18
Figure 10.....	19
Figure 11	20
Figure 12	20
Figure 13	21
Figure 14	22

List of Tables

Table 1.....	7
Table 2.....	12
Table 3.....	18

Introduction

Chronic low back pain (cLBP) is a complex condition with limited therapeutic options. Physical therapy, injection-based treatments, and pharmacologics (such as analgesics, anti-inflammatory drugs, muscle relaxants, etc.) are all options for treating chronic back pain¹. Among all of the treatments, opioid prescription for cLBP has increased and opioids are now the most commonly prescribed drug class². However, complications of opioid use in treating cLBP may include addiction and overdose-related mortality, which have risen in parallel with opioid prescription rates². In 2019, Eklund *et al* did a systematic review of increased opioid prescription in the US, which found that there is scant evidence of efficacy for opioids to treat chronic back pain¹. Loss of long-term efficacy could result from drug tolerance and emergence of hyperalgesia, where an individual's anticipation and perception of painful experiences plays a crucial part. Many studies have been done to understand the mechanism of individual pain experience. Various studies report that changes in individuals' expectation of pain affect their perception of pain^{3,4}. Eklund *et al.* also showed that positive expectation (expecting low pain) reduced self-reported pain level while negative expectation (expecting high pain) worsened the experience of pain¹. Nondeceptive placebo has demonstrated its efficiency in clinical practice and its effect may be mediated by expectation⁵. Better understanding underlying biological and psychological mechanisms might facilitate improved approaches for the management of cLBP and therapeutic outcomes. Given previous findings that expectation and anticipation play a major role in treatment outcomes^{3,4,6}, discovering the mechanism of cLBP anticipation and perception may inform stratification of patients to clinical pain management programs.

The goal of this study was to evaluate the association of brain structural and neuronal difference with severity of pain intensity and interference in participants with current cLBP. We analyzed structural brain magnetic resonance imaging (MRI) scans to study brain structure in

terms of difference in tissue volume in brain regions involved in pain processing and anticipation and functional magnetic resonance imaging (fMRI) to study neuronal activity using evoked pain paradigm¹⁶ in individuals with cLBP. fMRI is a noninvasive T2* relaxation -based MRI modality that is sensitive to local concentration of paramagnetic deoxyhemoglobin⁸; the blood-oxygen-level-dependent (BOLD) signal detected in fMRI reflects localized changes in blood flow and blood oxygenation level, an indirect measure of neuronal activity⁷. The evoked pain paradigm fMRI experiment used in this study involved randomized events of rest, visual cues for anticipated pain stimulus levels^{16,29,33} (i.e., low, high, or unknown), and delivery of pain stimulus at low or high pain levels. The evoked pain paradigm fMRI experiment design aimed to quantify neuronal activity of each individual during active pain anticipation and pain perception states.

Given that previous studies have found that cLBP is associated with both brain tissue volume and functional changes in certain brain structures^{9,10,11}, here we focused on structural and functional brain changes in the regions of interest (ROIs) previously implicated in pain processing and anticipation: insula cortex, anterior cingulate cortex, amygdala, and thalamus^{9,12,13,14,29}. The nucleus accumbens⁹ and substantia nigra¹⁵ were also included in this study because they are involved in cognitive and emotion processing. Studies have shown that patients with chronic pain have significant volume decrease in the right anterior insula cortex and left middle cingulate cortex¹⁸. Becerra *et al.* showed that noxious stimuli reliably produces nucleus accumbens¹⁹. Brain stem excluding substantia nigra was selected for its role in nociception and pain processing. The anterior cingulate and amygdala ROIs were chosen for their role in affective processing networks, the nucleus accumbens as representative of the ventral striatum, along with its common targets, the pallidum and substantia nigra, and lastly the caudate nucleus and putamen as representative of the dorsal striatum.

Through both volumetric and functional analysis of these regions, we expected to see structural difference correlated with varying severity of cLBP and subject-specific functional brain activation patterns when anticipating different levels of negative outcomes. We assessed the

degree to which an individual's neuronal activity patterns during low versus high pain stimulus and during known low versus high pain anticipation cues are distinguishable. Then we decoded each individual's anticipatory bias when presented with unknown visual cues. We aimed to assess the extent to which subject-specific intrinsic biases in pain perception and anticipation could explain the perceived severity of cLBP.

Methods

Participants

Subjects were recruited through current VA-funded trials in veterans with diagnosed cLBP from the Bay Area. Staff research associates contacted candidate participants to confirm their interest and conducted a 45-minute phone interview with each interested individual. The phone interview consisted of questions about their physical health, mental health, MRI safety, and substance use. Prior to the study participation, all subjects gave their written informed consent and had received clinical MRI as part of usual care. Subjects were excluded from the study if they: (1) used psychotropic medication within the last 30 days; (2) fulfilled DSM-IV criteria for alcohol/substance abuse or dependence within 30 days of study participation; (3) fulfilled DSM-IV criteria for lifetime bipolar or psychotic disorder; (4) had ever experienced a head injury; (5) had clinically significant comorbid medical conditions, such as cardiovascular and/or neurological abnormality, or any active serious medical problems requiring interventions or treatment; (6) had a history or current chronic pain disorder; (7) had irremovable ferromagnetic material; (8) were pregnant or claustrophobic; and (9) were left-handed.

Neuroimaging protocol

A 3T Siemens Skyra scanner equipped with a 32-channel head coil was used to acquire multimodal brain MRI data. The scanner allows for simultaneous multi-slice acquisition, or

multiband (MB) imaging, which generates full-brain, high-resolution acquisitions at a reduced repetition time. The following images were obtained for each subject: (1) 3D T1-weighted MP-RAGE for image registration, spatial normalization, brain parcellation, tissue segmentation (TR=2400 ms, TE=2.24 ms, flip angle=8°, FOV=256 mm*256 mm, 224 slices, 0.8*0.8*0.8 mm voxel); (2) two sets of task fMRIs using evoked pain paradigm (TR=820 ms, TE=35 ms, flip angle=58°, FOV=208 mm*208 mm, 72 slices, 2*2*2 voxel, MB=8). Field maps were acquired to correct for distortions, minimize registration error by using subject-specific templates and manual tweaking. Pulse oximeter was used on all participants to collect oxygen level of their blood. Acquisitions were time-locked to the onset of the task. The neuroimaging protocol was conducted the same across the entire clinical cohort.

Evoked pain paradigm fMRI experiment design

Before MRI, two temperatures between 42–46 °C were determined for each individual to elicit high pain and low pain through pain thresholding. Participants were then engaged in a sensory pain-anticipation task consisting of these two predetermined temperatures^{29,32,33} (Figure 1); the two temperatures elicited low pain (LP) and high pain (HP) sensations, respectively. Heat was delivered through a 9 cm² thermode (Medoc TSAII, Ramst-Yishai, Israel) on the participant's left forearm. Each trial began with a duration of 10 seconds (10 s) of anticipation initiated by a visual cue (**Figure 1**). Each visual cue was followed by painful stimulation (either HP or LP) for a period of 7 seconds and a random period of rest time (7-30s) before the next trial began. Two sessions of tasks were conducted. Each session contained seven HP cues (HP cue followed by HP stimulation), seven LP cues (LP cue followed by LP stimulation) and 14 uncertain cues (UN cue followed by either HP or LP stimulation at 50% probability). The order of visual cues of high pain and low pain was randomized separately for each session as illustrated in Figure 1, described elsewhere in full detail^{16,29,33}.

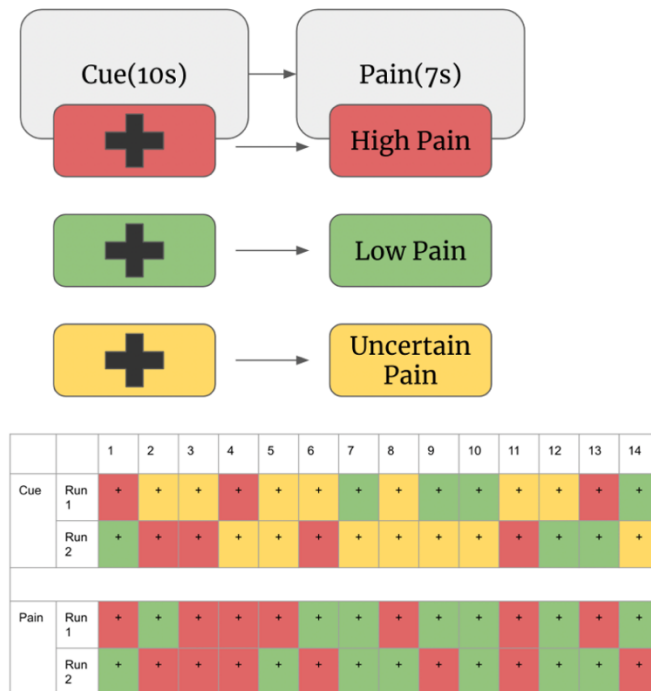


Figure 1: Illustration of task-based fMRI Design^{16,29,33}: Each trial began with a duration of 10 seconds (10s) of anticipation initiated by a visual cue. Each visual cue was followed by painful stimulation (either HP or LP) for a period of 7 s and a random period of rest time (7-30 s) before the next trial began. Two sessions of tasks were conducted. Every run contained 7 HP cues (HP cue followed by HP stimulation), 7 LP cues (LP cue followed by LP stimulation) and 14 uncertain cues (UN cue followed by either HP or LP stimulation at 50% probability). Yellow visual cues were followed by either HP or LP stimulation at 50% probability.

Structural image processing

Structural T1 MRI analysis was conducted on all 26 subjects through Advanced Normalization Tools (ANTs)¹⁷ to extract ROIs defined in an MNI standard space atlas (see Table 1). A total of 31 ROIs are chosen based on their prominent roles in pain prediction, processing, and relief. Accordingly, six ROIs were selected within the insula bilaterally: (1) posterior long gyrus, (2) anterior short gyrus, (3) middle short gyrus, (4) posterior short gyrus, (5) anterior inferior cortex, and (6) anterior long gyrus^{29,30}. The posterior insula, according to the current evidence, encodes objective thermosensory information, whereas the middle and anterior insula integrate thermosensory information with emotionally salient stimuli from all sensory modalities^{30, 31}.

Neuroanatomical and functional brain imaging studies also indicate that anterior insula integrates interoceptive, cognitive, and emotional experiences²⁹. Nine functionally relevant bilateral ROIs were selected: (1) anterior cingulate cortex, (2) amygdala, (3) nucleus accumbens, (4) caudate nucleus, (5) putamen, (6) pallidum, (7) substantia nigra, (8) pre-subgenual frontal cortex, and (9) thalamus. To extract these volumes, each subject's structural image was spatially normalized to a template image in standard MNI-152 space using nonlinear warping method from ANTs¹⁷. The 31 ROI masks which were defined in the MNI standard space were then registered onto each subject's T1 image to segment certain parts of the brain and measure the volume of each ROI. Individual intracranial volume (ICV) was calculated as well for volumetric analysis. Specifically, the relative ICV-to-template ratio was determined by calculating the determinant of the affine transformation matrix acquired from the ANTs registration. The ICV-to-template ratio was then multiplied by the ICV of the MNI-152 template to calculate a total ICV value per subject. Spatial normalization and ROI segmentation results were inspected visually for accuracy.

Table 1: Regions of interest: 31 ROIs are chosen based on their prominent roles in pain prediction, processing, and relief. Insula, basal ganglia, cingulate cortex, frontal cortex, amygdala, brain stem and thalamus are the main areas that we focus on.

Insula L and R	Insula posterior long gyrus	Basal Ganglia L and R	Caudate nucleus
	Insula anterior short gyrus		Nucleus accumbens
	Insula middle short gyrus		Putamen
	Insula posterior short gyrus		Pallidum
	Insula anterior inferior cortex		Substantia nigra
	Insula anterior long gyrus	Frontal Cortex L and R	Pre subgenual frontal cortex
Cingulate L and R	Anterior cingulate gyrus		
Amygdala (L and R) and Brainstem	Brain stem excluding substantia nigra	Thalamus L and R	Thalamus
	Amygdala		

Task-Based fMRI image processing

MATLAB-based CONN functional connectivity toolbox⁶ was used to preprocess the task-based fMRI images. Preprocessing included: (1) functional realignment and unwarp, (2) functional center to (0,0,0) coordinates, (3) functional slice-timing correction, (4) functional outlier detection, (5) functional direct segmentation and normalization, and (6) functional smoothing. Spatial noise reduction with masked ICA (Independent Component Analysis) was utilized for temporal noise reduction. Spatial masking was implemented before data smoothing, which helped reduce the contamination of brainstem signals with physiological noise from neighboring regions. For the functional outlier detection (step 4), the intermediate settings were chosen with 97th percentile in the normative sample. For segmentation and normalization (step 5), default tissue probability maps were used for the simultaneous segmentation of gray, white matter and cerebrospinal fluid (CSF) and Montreal Neurological Institute (MNI) coordinate normalization. The smoothing kernel

used in the functional smoothing (step 6) was 4 mm full-width half maximum (FWHM). Next, denoising was performed on the functional data. Here, linear detrending and regression of the confounding effects of realignment and scrubbing was completed. De-spiking was implemented before regression and a band pass filter of [0.008 Hz, infinity] was applied after regression.

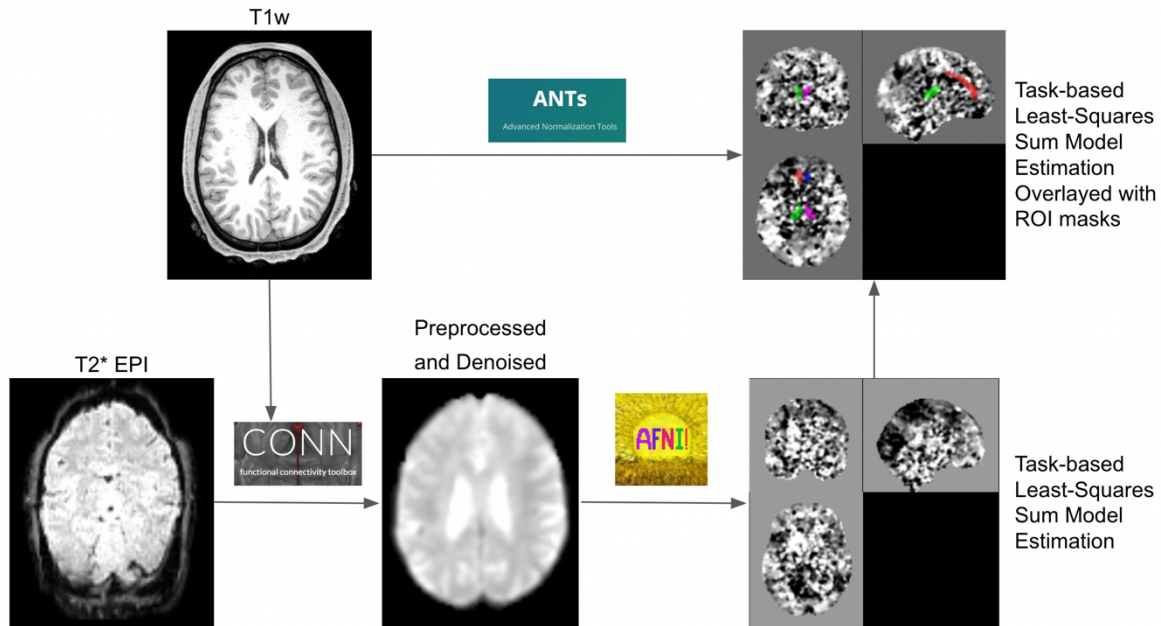


Figure 2: Illustration of fMRI image processing flow: T1w images were input into Advanced Normalization Tool (ANTs) to extract ROI masks for each individual. BOLD task fMRI images were registered with T1w images for CONN pre-processing and denoising. The images were then inputted into the Analysis of Functional Neuroimages (AFNI) to build individual activation maps. ROI masks were applied to the individual activation maps for a multimodal image processing fusion to create a matrix of 31 ROIs as rows and 28 events as columns.

Further analysis on preprocessed task fMRI data was conducted using the Analysis of Functional NeuroImages (AFNI) software package²⁰. To reduce the false positives caused by signal overlapping in a short amount of time, time series data was fit using the AFNI 3dLSS, which applies a least-squares-sum model estimation to the individually modulated time-series data to deconvolve BOLD activation (3dDeconvolve)²¹. Masks of selected 31 ROIs created in T1 image space of each subject via ANTs processing were applied to the average BOLD activation maps for each anticipation and pain stimulus period (N=28) using AFNI 3dROIstats²² to extract the mean

activation in each ROI. An ROI activation map for each subject during pain perception and pain anticipation period was then created separately.

Clinical Pain Severity Assessment

The Pain, Enjoyment, General activity (PEG-3) Scale²⁸ is a self-reported clinical severity assessment of pain intensity and interference of participants' daily life. The PEG questionnaire is composed of three questions:

1. What number best describes how, during the past week, pain has interfered with your enjoyment of life?
2. What number best describes your pain on average in the past week?
3. What number best describes how, during the past week, pain has interfered with your general activity?

Participant answers to these three questions were provided on a scale of 0 to 10, where 0 is "Does not interfere" and 10 is "Completely interferes" for questions 1 and 3. For the second question, 0 is "No pain" and 10 is "Pain as bad as you can imagine". The overall pain score is calculate as the average of these three item level scores, higher overall score indicating greater pain severity.

Statistical Analysis

Aim 1: To assess to what extent patient-reported pain outcome measure (PEG-3) is associated with regional tissue volumes of brain regions implicated in pain processing and anticipation in patients with cLBP

The single ROI volumes were compared with individuals' PEG scores through linear regression to test their associations. Intracranial volume, age and sex were included in the

regression model as covariates. Holm's correction was used to correct the results for multiple comparisons. R^2 delta (of the ROI volume) was estimated by subtracting the R^2 of regression model containing ICV, age and sex from the total R^2 of the regression model containing ROI volume, ICV, age and sex. Effect size and confidence interval for each ROI were determined using the effect size package²⁶ in R.

Aim 2 : To determine the extent to which within-subject neural response during high pain vs low pain stimulus are distinguishable in patients with cLBP. To evaluate the association between individual neuronal brain activity during pain perception and patient-reported pain outcome measures (PEG-3)

For each participant , the average activation from each ROI during pain stimulus trials were used as independent predictors in a logistic regression analysis with Least Absolute Shrinkage and Selection Operator (LASSO) to assess whether their neural activations during high pain and low pain stimulus are distinguishable. With 31 ROIs (independent predictor variables) but only 28 events (dependent outcome observations), regularized logistic regression allows us to search for a sparse regression model fit³⁵. To balance the bias in predictor selection and variance in predictor load, we used a leave one out cross validation method to select the LASSO tuning parameter³⁶. A major advantage of LASSO is that it is a combination of both shrinkage and selection of variables and optimal tuning in LASSO regularization allows for accurate and consistent discrimination between single-subject neurobiological patterns of low- and high-pain perception and anticipation. LASSO modeling was performed using glmnet package³⁸.

The model for each single subject to distinguish between high pain and low pain brain activation was assessed using receiver operating characteristic (ROC) analysis, and described by area under the curve (AUC). A permutation test was run to determine the accuracy of the LASSO models.

Similar to Aim1, the individual ROI average activation from all trials during pain perception was compared with individuals' PEG scores through linear regression to evaluate their associations. The linear regression models didn't include ICV, age and sex since we don't expect them to be confounding effects to the association. All analyses were done in R studio software³⁹.

Aim 3 : To determine the extent to which within-subject neural responses during high pain vs low pain anticipation cues are distinguishable in patients with cLBP and decode their anticipatory bias when they were presented with unknown visual cues. To evaluate the association between individual neuronal brain activity during unknown pain anticipation, anticipatory bias and patient-reported pain outcome measures (PEG-3)

The activation in every ROI during certain pain level anticipation cue trials were used to build individual pain anticipation classifiers using logistic regression modeling with LASSO regularization. LASSO modeling mirrored the approached used in Aim 2. LASSO was performed on a single-subject basis in which the training set contains neural activations from 31 ROIs simultaneously as independent predictors during 14 certain anticipation trials as high pain (HP) anticipation cue and low pain (LP) anticipation cue are the dependent outcomes, and then target data to decode would be the neural activation during the 14 uncertain anticipation cue trials.

With the 14 uncertain anticipation cue trials brain activation being input into the model as test data, predictions were made based on if the neural patterns when presented with unknown visual cues were more similar to the one when presented with high pain visual cue or low pain visual cue. The LASSO probabilistic prediction results for all 14 unknown cue trials were then averaged to determine overall intrinsic anticipatory bias of each individual separately. Accordingly, participants with a low average probability (< 0.5) of anticipating HP during uncertain cues are interpreted as the ones with positive anticipatory bias, and the ones with a high average probability (≥ 0.5) of anticipating HP during uncertain clues are the negative anticipatory bias. Both binomial prediction and the predicted probability of anticipating high pain were reported.

Similar to Aims 1 and 2, the association between PEG-3 scores and neuronal activation averaged over all trials with known anticipation visual cues as well as decoded anticipatory bias and the PEG-3 overall scores were assessed through linear regression. The linear regression models didn't include ICV, age and sex since we don't expect them to be confounding effects to the association.

Results

Clinical characteristics of the cohort

Table 2: Cohort characteristics at baseline

Baseline N	26 subjects
Age (years)	45.36 ± 12.80
Sex (F%)	17 females 65.4%
Race/ethnicity	76% White, 16% Asian, 8% Black or African American; 1 subject - White and Asian
Education	8% High school complete, 16% Associate's or technical degree, 48% College degree, 28% Doctoral or postgraduate degree

Data was collected from 26 subjects for the current study; baseline demographic characteristics of the study cohort are reported in Table 3.

Clinical Assessment- PEG Score

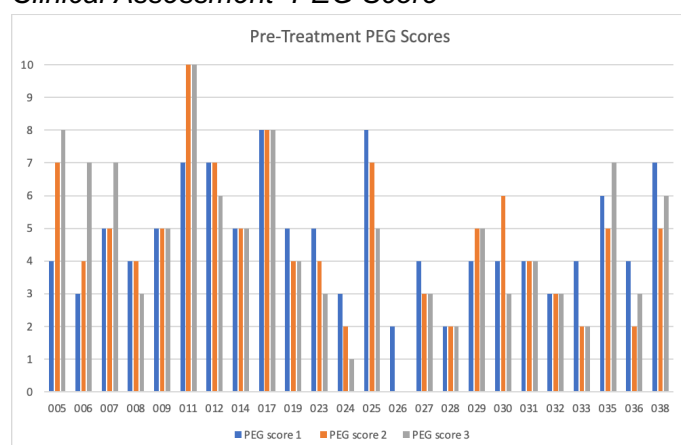


Figure 3: Cohort PEG scores at baseline: PEG scales measure participants' daily experience with their chronic low back pain.

Baseline (N=26) PEG-3 scores of the study participants are shown in **Figure 3**.

Volumetric analysis

The volumes of both left insula middle short gyrus and right anterior inferior cortex volumes were associated with worse PEG Question 1 scores (**Figure 4** and **Figure 5**). The volumes of both left and right anterior cingulate gyrus were found to be negatively associated with PEG Questions 2 and 3 scores. When compared with average answers to all three questions, both left and right anterior cingulate gyrus volumes were shown to be negatively associated, meaning that the larger volume of both structures is associated with a relatively lower self-report score on PEG scale. The structural brain visualization was acquired with the BrainNet Viewer²⁷, as shown in **Figure 6**.

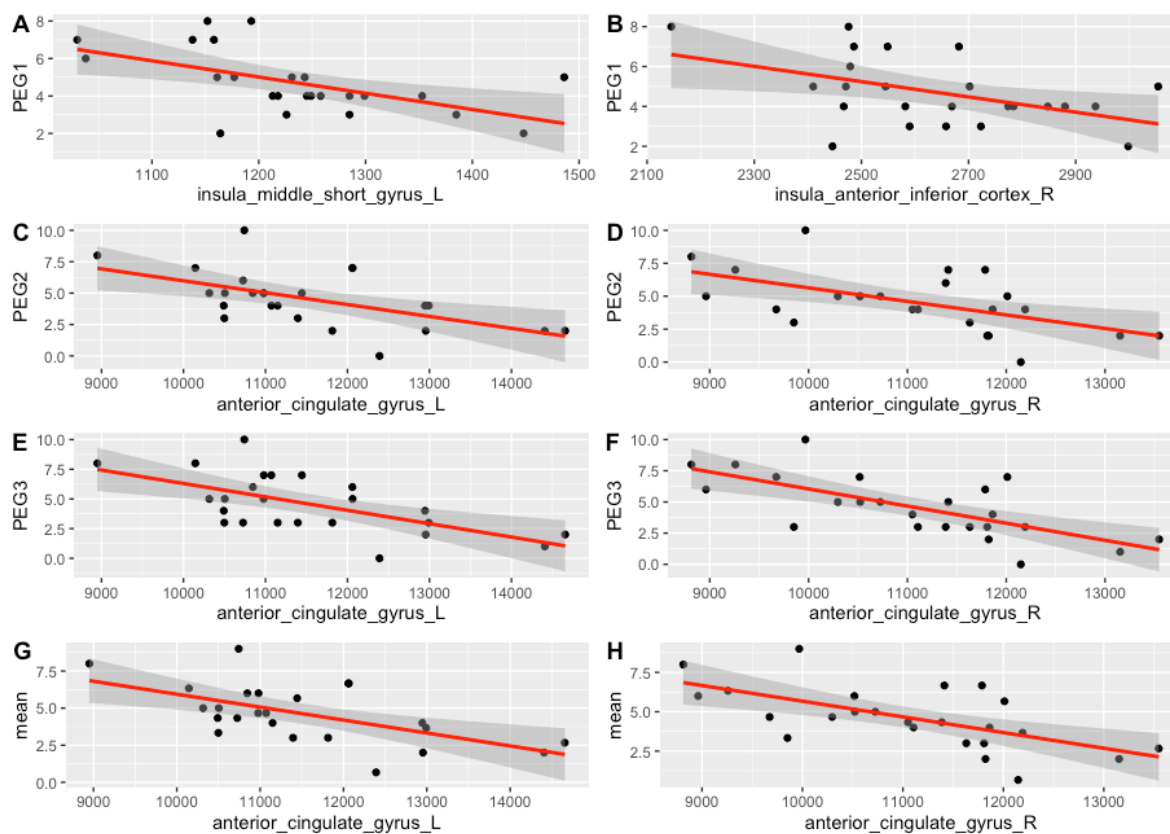


Figure 4: Association between PEG scores and certain ROI volume: Among all the linear regression models that

were built, these eight models have a R^2 delta over 0.25. All of them show a negative association between self-report PEG scores vs. certain ROI volume

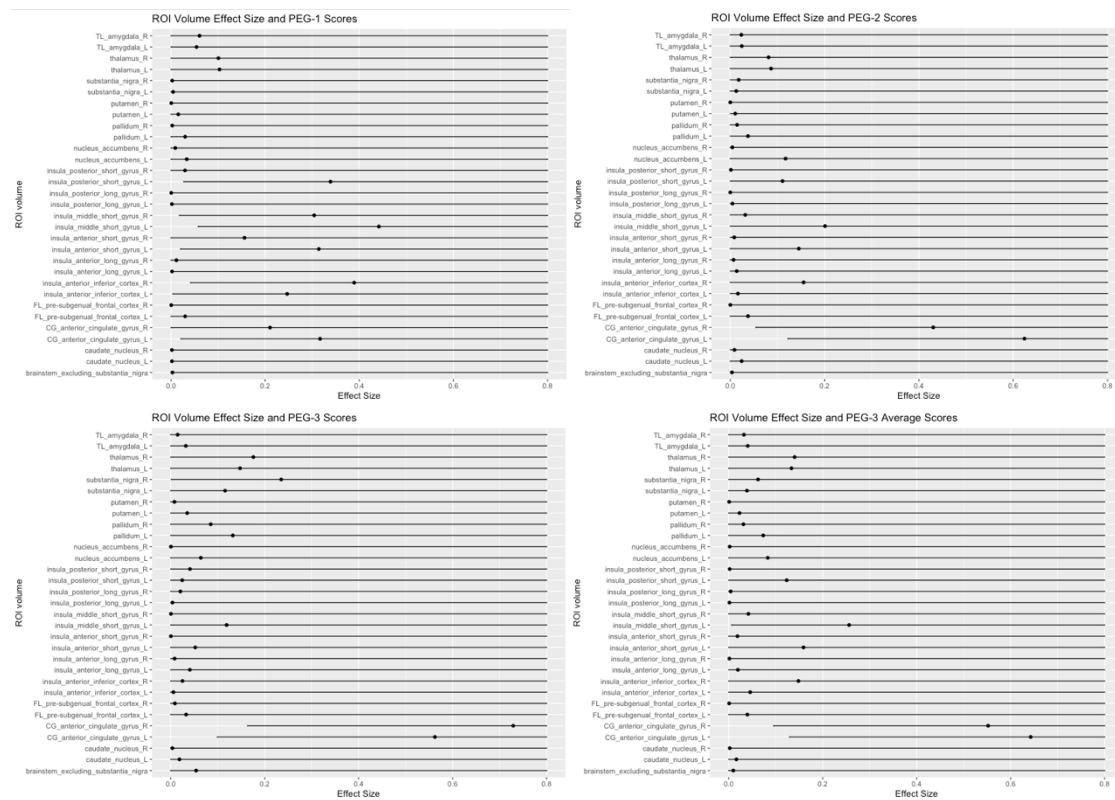
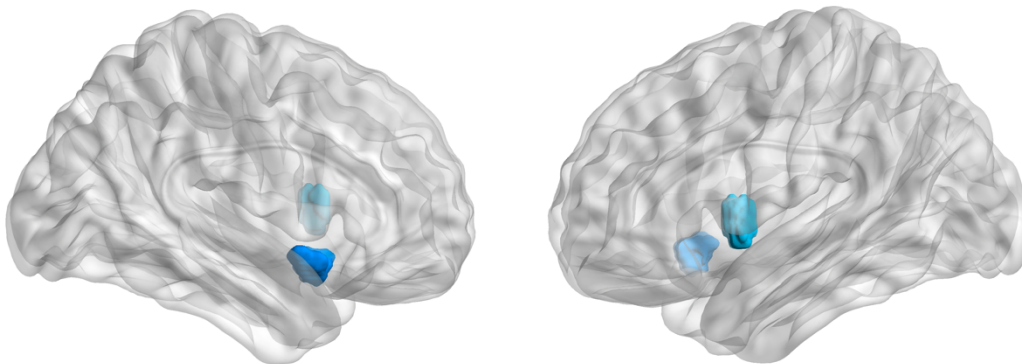
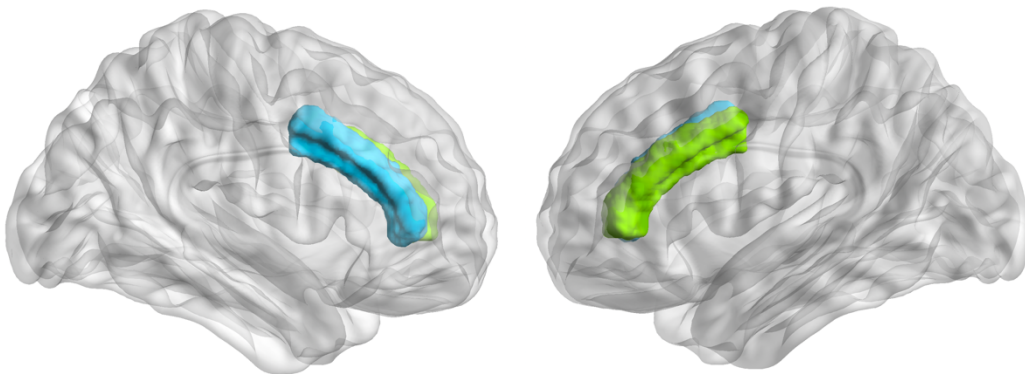


Figure 5: Effect size and 95% confidence level of all ROI volume linear regression models. Volumes of left insular middle short gyrus and right insula anterior inferior cortex were associated with PEG-1 scores. Volumes of both left and right anterior cingulate cortex were shown to associated with PEG-2, 3 and average scores.

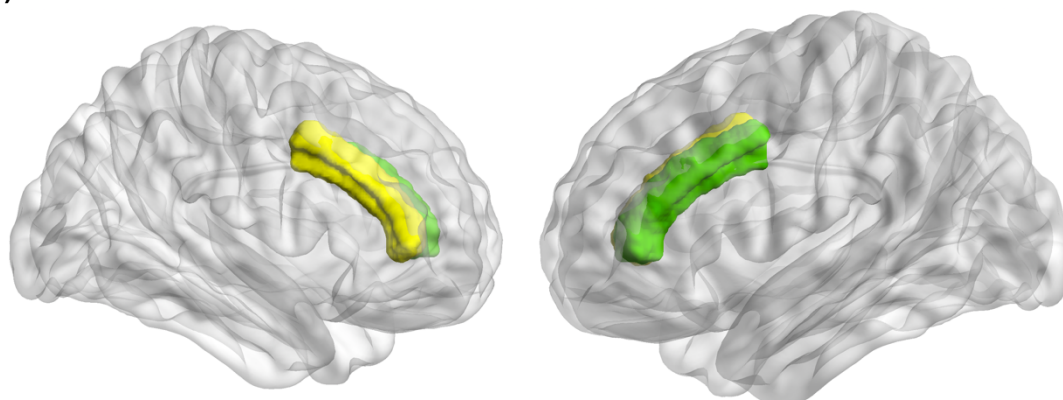
a)



b)



c)



d)

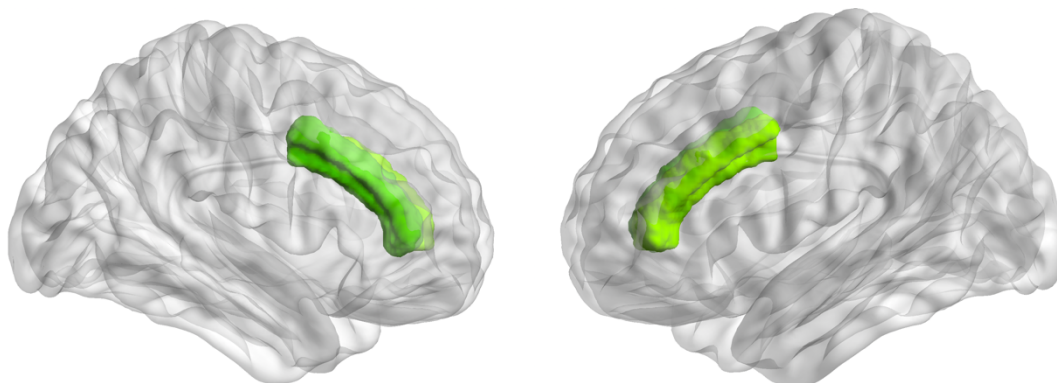




Figure 6: Effect size visualization of ROIs where volume was associated with PEG-3 scores.

Low Accuracy of Lasso Models When Differentiating Between High Pain and Low Pain Neural Response Patterns

In differentiating high pain and low pain brain activation at single subject level, LASSO logistic regression models performed modestly with an average area under the curve (AUC) of 0.773 ± 0.206 , with 0.65 ± 0.179 accuracy, 0.747 ± 0.136 sensitivity and 0.543 ± 0.262 specificity across all participants. Among all the ROIs that were input into LASSO models as predictors (**Figure 7**), left posterior long gyrus (37.5%), right posterior short gyrus(33.3%), right middle short gyrus (37.5%), and right anterior long gyrus (33.3%) within the insula contributed to the differentiation between high pain and low pain stimulus the most frequently across the subject-specific LASSO logistic regression models. Right pallidum (37.5%) and right substantia nigra (37.5%) also played a role into perceiving high pain vs. low pain. The structures that were shown to contribute to differentiating between high pain and low pain were visualized in **Figure 8**.

Four linear regression models (**Figure 9**) were also built to evaluate the association between average ROI activation during pain perception and reported PEG scores. All the effect sizes were too small to conclude whether there was an association between regional activation during pain stimulus and the PEG scores.

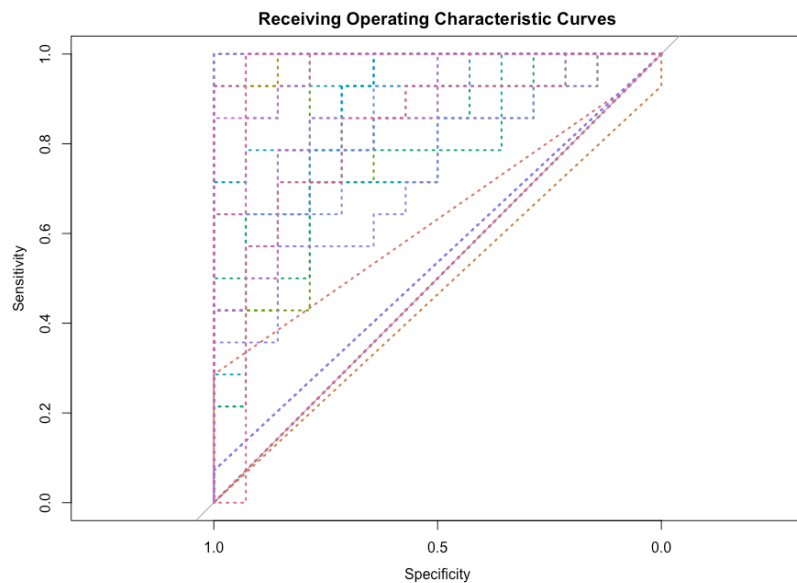


Figure 7: Receiving Operating Characteristic Curves for Pain Perception. Dashed lines are ROCs of individual subject-specific LASSO models in separating high pain and low pain perception.

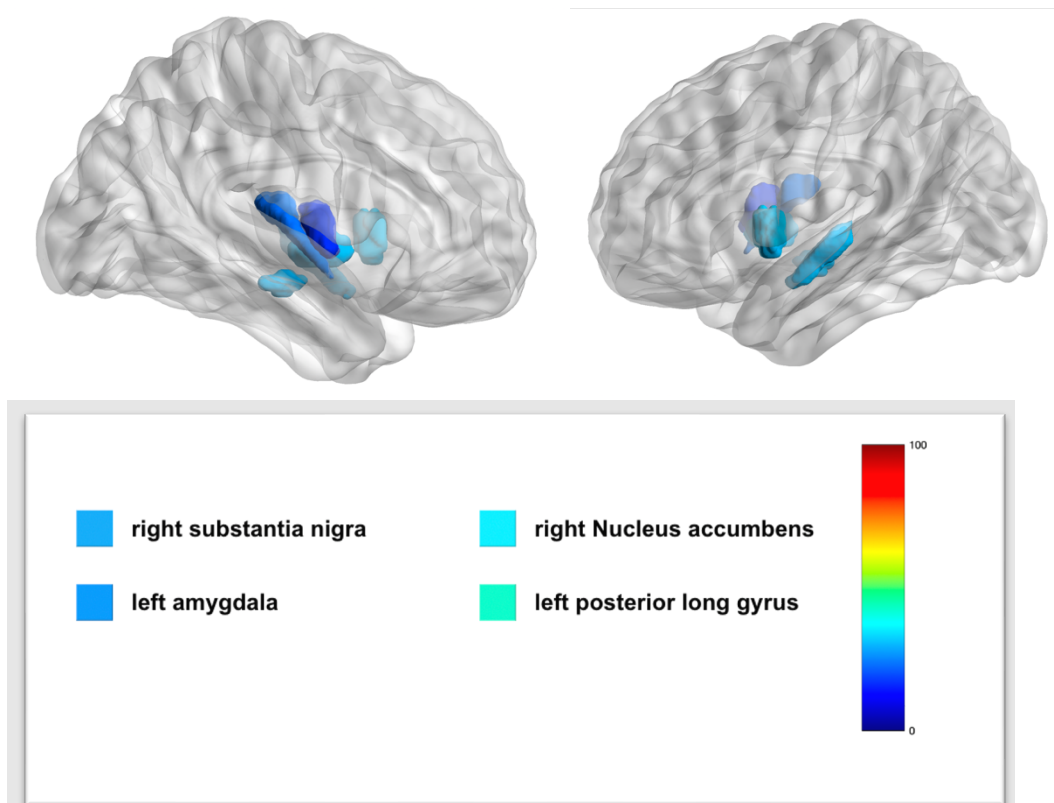


Figure 8: ROIs that contribute to differentiating between high pain and low pain stimulus

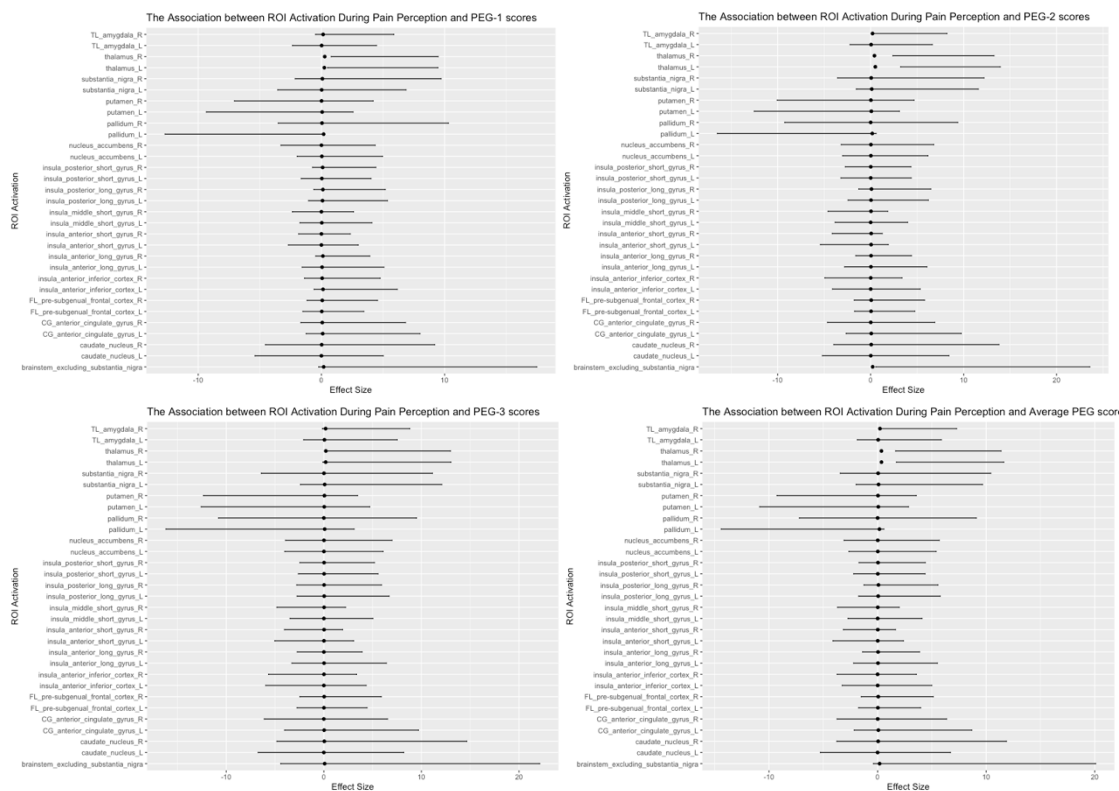


Figure 9: Association between ROI activation during pain perception and patient-reported PEG scores

Table 3: Single subject LASSO logistic regression model accuracy in differentiating neuronal activity during high vs low pain stimulus (i.e., PAIN Model) and during high vs low pain anticipation cues (i.e., ANT Model)

Subject ID	PAIN Model Accuracy	ANT Model Accuracy
1	0.57	0.71
2	0.34	0.79
3	0.68	0.56
4	0.5	0.64
5	0.73	0.79
6	0.5	0.56
7	1	0.5
8	0.56	1
9	0.5	1
10	0.75	0.93
11	0.62	0.86
12	1	0.71
13	0.5	1
14	0.75	0.57
15	1	1
16	1	0.64
17	0.75	0.56
18	0.41	1

19	0.61	0.5
20	0.64	0.5
21	0.79	1
22	0.5	1
23	0.54	0.71
24	0.66	0.5
25	0.5	0.71
26	0.41	0.79

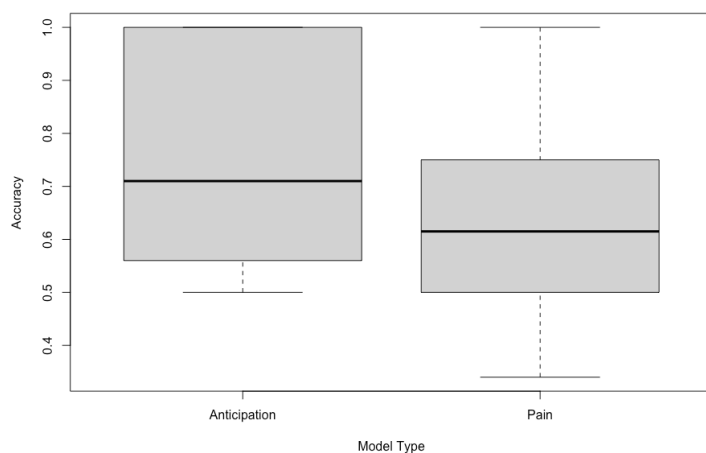


Figure 10: Anticipation and pain perception LASSO model accuracy comparison

Higher Accuracy of Single LASSO Model When Decoding Participants' Anticipatory Bias

In differentiating brain activation during known high vs low pain anticipation cues at single subject level, LASSO logistic regression models performed at an average AUC of 0.861 ± 0.218 , with 0.75 ± 0.21 accuracy, 0.828 ± 0.127 sensitivity, and 0.546 ± 0.321 specificity across all participants (**Figure 11**). Among all ROIs considered in these LASSO models, insula was the most frequent contributor (72% of the subjects) to differentiate the high pain stimulus anticipation and low pain stimulus anticipation. Within the insula, left posterior long gyrus (52%) were recruited during the anticipation of pain. Right nucleus accumbens (48%), left amygdala (44%), and right substantia nigra (42%) also were shown to play a role in anticipating negative outcomes (**Figure 12**).

Table 3 shows the accuracy of LASSO models built for 26 subjects and **Figure 10** shows the accuracy comparison between anticipation and pain perception LASSO models.

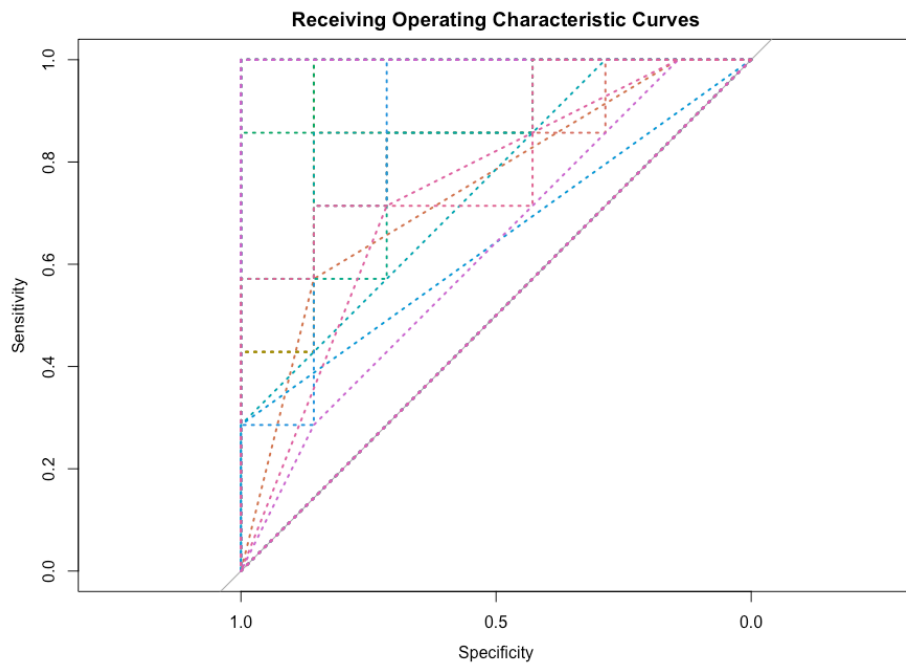
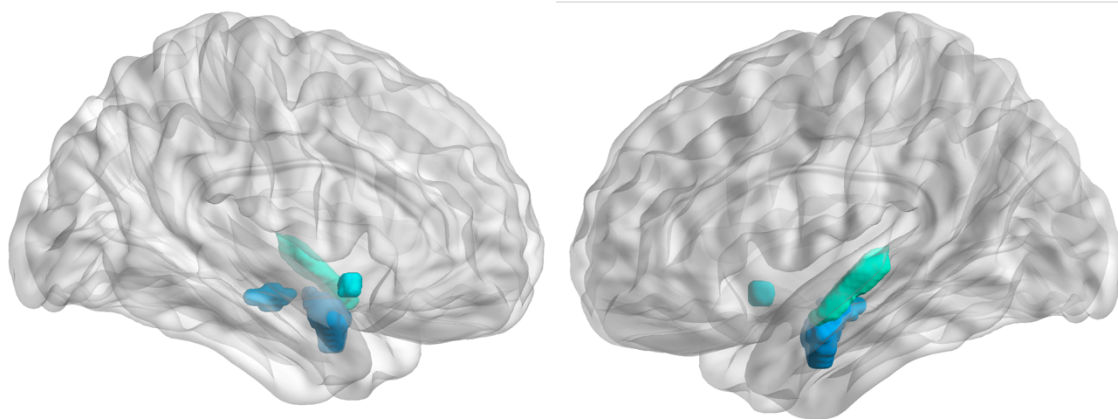


Figure 11: Receiving Operating Characteristic Curves for Pain Perception. Dashed lines are ROCs of individual subject-specific LASSO models in separating high pain and low pain perception.



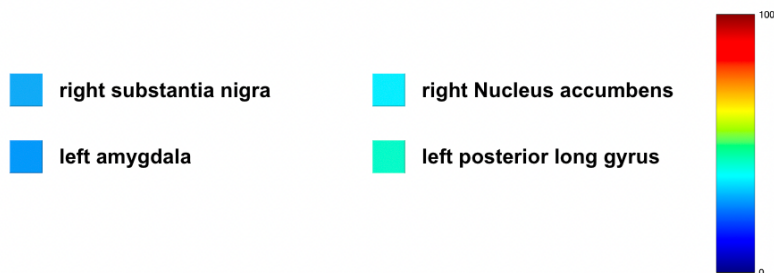


Figure 12: ROIs that contribute to differentiating between high pain and low pain anticipation.

Individual anticipatory bias based neuronal activation during the unknown pain anticipation visual cues was decoded for each participant separately using their own subject-specific LASSO models (**Figure 13**). Twenty out of the 26 subjects (76.9%) were stratified as presenting with a negative anticipatory bias while the six (23.07%) were recognized as having positive anticipatory bias based on their subject specific LASSO model.

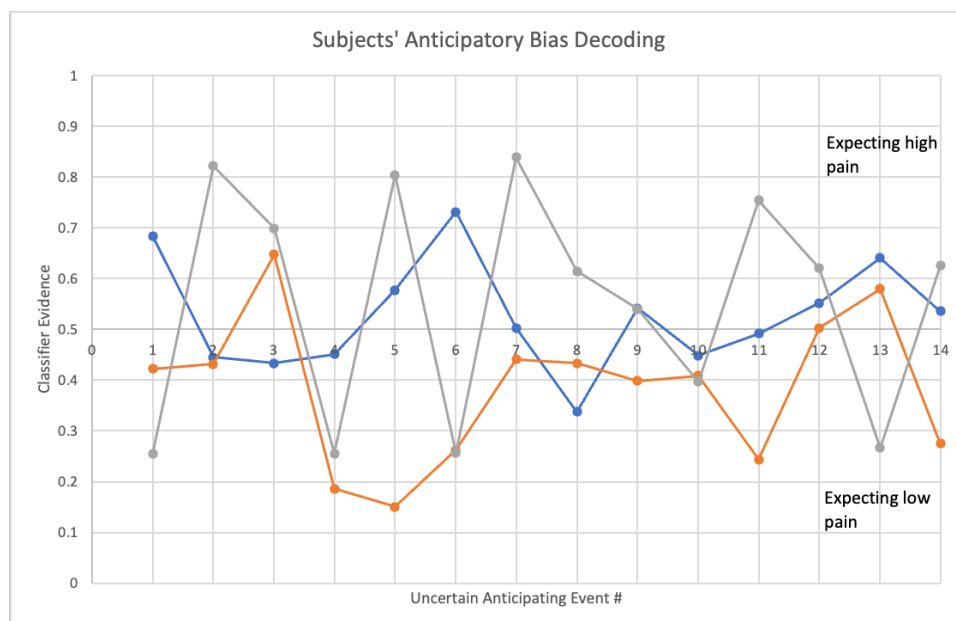


Figure 13: Decoding the bias of three subjects. Based on the probabilistic prediction made by the subject-specific LASSO model, individual's brain activation during unknown visual cues is classified as more similar to the one when presented with high pain visual cues or to the one when presented with low pain visual cues. In this case, the subject with orange trendline shows that they are expecting high pain for four trials and low pain for the other ten trials. The subject with blue trendline is expecting high pain for seven trials and low pain for the rest seven trials. The subject with gray trendline is expecting high pain for nine trials and low pain for the rest five trials.

Four linear regression models were built to evaluate the association between average ROI activation during pain anticipation and reported PEG scores (**Figure 14**). It was shown that all the effect sizes were too small to conclude whether there was an association between certain ROI activation and PEG scores during the pain anticipation period. Participant average PEG scores were also input with their anticipatory bias for further analysis using linear regression. The p-value for the model is 0.262 and R^2 is 0.03, indicating that there is no significant relationship between how participants experiencing chronic low back pain in their daily life versus their anticipatory bias during pain-anticipation paradigm.

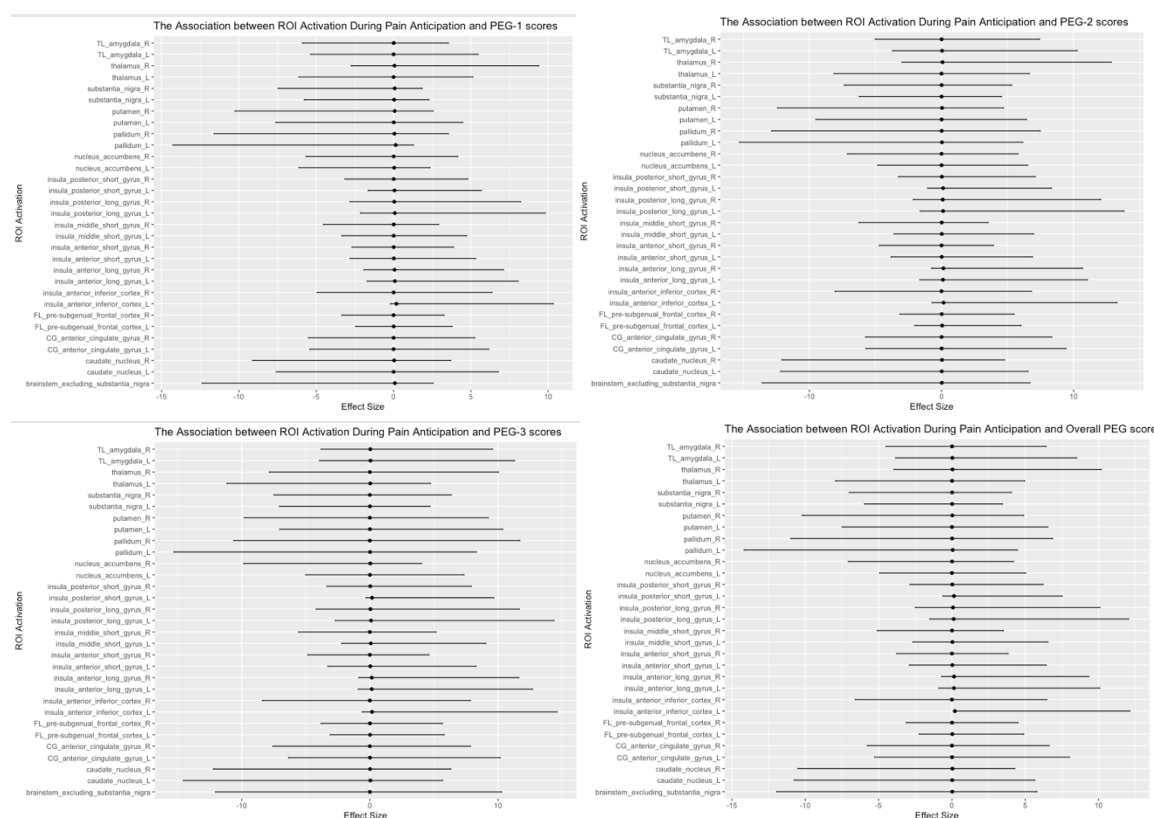


Figure 14: The association between ROI activation during pain anticipation and patient-reported PEG scores

Discussion

In this study, we aimed to evaluate the association of brain structural and neuronal alterations with severity of pain intensity and interference in participants with current cLBP. Our

major findings are as follows: 1) multivariate analysis showed that individual perception of cLBP is negatively correlated with left insula middle short gyrus, right insula anterior inferior cortex, bilateral anterior cingulate cortex volumes, 2) there was relatively lower accuracy when using individual LASSO models to separate individual neural patterns during high and low pain stimulus and there was no significant association between ROI neuronal activation during pain perception and PEG scores, 3) using subject-specific LASSO modelling showed relatively higher accuracy when classifying individual neuronal activity when presented with known visual cues of anticipated pain. We decoded each participants neuronal activity during unknown visual cues of anticipated pain as the classifier determines if an individual's brain activation was more similar to the one when anticipating high pain or low pain outcomes; there was no significant association between ROI neuronal activation during pain anticipation and overall PEG scores as well as individual anticipatory bias and overall PEG scores. These findings add valuable information to the current understanding of pain anticipation and perception and may help with the further research on chronic low back pain patients' different levels of experience.

In volumetric analysis, psychiatric diseases and other health conditions are common comorbidities of cLBP, and could affect the size of the brain structures^{23,24}, it would be useful to add these conditions to the study for more in-depth analysis of the correlation between brain volume and individual daily experience with chronic low back pain. Previous studies have found that the anterior part of the insula plays a role in the anticipation of painful stimulus^{10,12}. We, along with Greenberg *et al.*²⁵, have observed the recruitment of middle or anterior part of the insula when anticipating negative outcomes. This indicates that there might be more than a few parts of the brain that may be correlated with anticipation of negative outcomes. Perhaps including more brain structures, such as lower brain stem regions, may be informative since cognitive and emotional processing occur in this region³⁰.

One of the limitations of this study is the relatively small sample size, which causes group analysis to have big residual errors. Another limitation is that within the cohort, there might be a

large amount of heterogeneity, which causes the LASSO model accuracy to vary. Additionally, the number of predictors are more than the number of observations, which might result in predictors being overly penalized in the LASSO model. Further, during the anticipation period, the prior high- and low-pain stimulus might affect participants' anticipation tendency in the following trial. Since these effects were not controlled for in the study, they could cause a biased result.

Future studies could include more participants. Having a control cohort and a cLBP cohort can also help to control the heterogeneity of the entire cohort. Other regularization methods such as ElasticNet and Ridge could be used to compare the accuracy of the logistic regression models. Moreover, when computing for anticipatory bias, the model could include the prior pain stimulus level as one covariate to evaluate the effect. Although task fMRI is the gold standard to study neuronal activity, expertise and equipment required to run specialized task fMRI studies hinders its scalability and operationalization in clinical practice and in multi-center research studies. Using supervised machine learning models predictive of each subject's anticipation bias phenotype from their resting state fMRI data can be more easily accessed in clinical settings.

Overall, we explored the structural difference correlated with various severity of cLBP and subject-specific functional brain activation patterns when perceiving and anticipating different levels of negative outcomes. We also assessed the degree to which an individual's neuronal activity patterns during low versus high pain stimulus and during known low versus high pain anticipation cues are distinguishable. We decoded individuals' anticipatory bias when presented with unknown visual cues. Lastly, we evaluated the association between ROI neural activation during pain perception, anticipation, individual anticipatory bias and patient-reported PEG scores. Objective imaging-based biomarkers of intrinsic anticipation bias phenotyping such as those presented in this study may be applicable in clinical settings in stratifying patients with cLBP from which they might benefit the most.

References

1. Eklund A, De Carvalho D, Pagé I, Wong A, Johansson MS, Pohlman KA, Hartvigsen J, Swain M. Expectations influence treatment outcomes in patients with low back pain. A secondary analysis of data from a randomized clinical trial. *Eur J Pain*. 2019 Aug;23(7):1378-1389. doi: 10.1002/ejp.1407. Epub 2019 May 20. PMID: 31034102; PMCID: PMC6767754.
2. Deyo RA, Von Korff M, Dührkoop D. Opioids for low back pain. *BMJ*. 2015;350:g6380. Published 2015 Jan 5. doi:10.1136/bmj.g6380.
3. Wiech, K., Vandekerckhove, J., Zaman, J., Tuerlinckx, F., Vlaeyen, J. W., & Tracey, I. Influence of prior information on pain involves biased perceptual decision-making. *Current Biology* 24, 15 (2014).
4. Leknes, S., Berna, C., Lee, M. C., Snyder, G. D., Biele, G., & Tracey, I. The importance of context: When relative relief renders pain pleasant. *Pain* 154, 402-410 (2013).
5. Wei H, Zhou L, Zhang H, Chen J, Lu X, Hu L. The Influence of Expectation on Nondeceptive Placebo and Nocebo Effects. *Pain Res Manag*. 2018 Mar 19;2018:8459429. doi: 10.1155/2018/8459429. PMID: 29755621; PMCID: PMC5884148.
6. Ward S, Guest C, Goodall I, Bantel C. Practice and bias in intraoperative pain management: results of a cross-sectional patient study and a survey of anesthesiologists. *J Pain Res*. 2018;11:561-57 <https://doi.org/10.2147/JPR.S153857>
7. Hillman EM. Coupling mechanism and significance of the BOLD signal: a status report. *Annu Rev Neurosci*. 2014;37:161-81. doi: 10.1146/annurev-neuro-071013-014111. PMID: 25032494; PMCID: PMC4147398.
8. Ogawa S, Lee TM, Kay AR, Tank DW. Brain magnetic resonance imaging with contrast dependent on blood oxygenation. *Proc Natl Acad Sci U S A*. 1990 Dec;87(24):9868-72. doi: 10.1073/pnas.87.24.9868. PMID: 2124706; PMCID: PMC55275.

9. Yang S, Chang MC. Chronic Pain: Structural and Functional Changes in Brain Structures and Associated Negative Affective States. *Int J Mol Sci*. 2019 Jun 26;20(13):3130. doi: 10.3390/ijms20133130. PMID: 31248061; PMCID: PMC6650904.
10. Ng SK, Urquhart DM, Fitzgerald PB, Cicuttini FM, Hussain SM, Fitzgibbon BM. The Relationship Between Structural and Functional Brain Changes and Altered Emotion and Cognition in Chronic Low Back Pain Brain Changes: A Systematic Review of MRI and fMRI Studies. *Clin J Pain*. 2018 Mar;34(3):237-261. doi: 10.1097/AJP.0000000000000534. PMID: 28719509.
11. Feitosa, A.A., Amaro Junior, E., Sanches, L.G. et al. Chronic low back pain and sick-leave: a functional magnetic resonance study. *Adv Rheumatol* 60, 46 (2020). <https://doi.org/10.1186/s42358-020-00146-4>
12. Ivo R, Nicklas A, Dargel J, Sobottke R, Delank KS, Eysel P, Weber B. Brain structural and psychometric alterations in chronic low back pain. *Eur Spine J*. 2013 Sep;22(9):1958-64. doi: 10.1007/s00586-013-2692-x. Epub 2013 Feb 8. PMID: 23392554; PMCID: PMC3777081.
13. Asada, Masako^{a,b}; Shibata, M^{a,c,d,*}; Hirabayashi, Naoki^{a,c}; Ohara, Tomoyuki^{a,e}; Furuta, Yoshihiko^{a,f}; Nakazawa, Taro^{a,e}; Honda, Takanori^a; Hata, Juna^{d,f}; Hosoi, Masako^c; Sudo, Nobuyuki^c; Yamaura, Ken^b; Ninomiya, Toshiharu^d. Association between chronic low back pain and regional brain atrophy in a Japanese older population: the Hisayama Study. *PAIN*: November 2022 - Volume 163 - Issue 11 - p 2185-2193 doi: 10.1097/j.pain.0000000000002612
14. Apkarian AV, Sosa Y, Sonty S, Levy RM, Harden RN, Parrish TB, Gitelman DR. Chronic back pain is associated with decreased prefrontal and thalamic gray matter density. *J Neurosci*. 2004 Nov 17;24(46):10410-5. doi: 10.1523/JNEUROSCI.2541-04.2004. PMID: 15548656; PMCID: PMC6730296.
15. Borsook D, Upadhyay J, Chudler EH, Becerra L. A key role of the basal ganglia in pain and analgesia--insights gained through human functional imaging. *Mol Pain*. 2010 May 13;6:27. doi: 10.1186/1744-8069-6-27. PMID: 20465845; PMCID: PMC2883978.

16. Kadlec et al. BOLD Decoding of Individual Pain Anticipation Biases During Uncertainty doi: <https://doi.org/10.1101/675645>
17. Avants, B. B., Tustison, N. J., Song, G., Cook, P. A., Klein, A., & Gee, J. C. A reproducible evaluation of ANTs similarity metric performance in brain image registration. *NeuroImage* 54, 2033-2044 (2011).
18. Ikeda E, Li T, Kobinata H, Zhang S, Kurata J. Anterior insular volume decrease is associated with dysfunction of the reward system in patients with chronic pain. *Eur J Pain*. 2018 Jul;22(6):1170-1179. doi: 10.1002/ejp.1205. Epub 2018 Mar 5. PMID: 29436061.
19. Becerra L, Breiter HC, Wise R, Gonzalez RG, Borsook D. Reward circuitry activation by noxious thermal stimuli. *Neuron* 2001;32:927–46.
20. Cox, R. W. AFNI: Software for analysis and visualization of functional magnetic resonance neuroimages. *Computers and Biomedical Research* 29, 162-173 (1996).
21. Whitfield-Gabrieli, S., & Nieto-Castanon, A. N. NITRC: CONN: Functional connectivity toolbox: Tool/Resource Info. Retrieved from <http://www.nitrc.org/projects/conn> (n.d.).
22. B. Douglas Ward. Deconvolution Analysis of fMRI Time Series Data. AFNI 3dDeconvolve Documentation, Medical College of Wisconsin, May 2002.
23. Reite M, Reite E, Collins D, Teale P, Rojas DC, Sandberg E. Brain size and brain/intracranial volume ratio in major mental illness. *BMC Psychiatry*. 2010 Oct 11;10:79. doi: 10.1186/1471-244X-10-79. PMID: 20937136; PMCID: PMC2958994.
24. Boublay N, Bouet R, Dorey JM, Padovan C, Makaroff Z, Fédérico D, Gallice I, Barrellon MO, Robert P, Moreaud O, Rouch I, Krolak-Salmon P; Alzheimer's Disease Neuroimaging Initiative. Brain Volume Predicts Behavioral and Psychological Symptoms in Alzheimer's Disease. *J Alzheimers Dis*. 2020;73(4):1343-1353. doi: 10.3233/JAD-190612. PMID: 31903989.
25. Greenberg T, Carlson JM, Rubin D, Cha J, Mujica-Parodi L. Anticipation of high arousal aversive and positive movie clips engages common and distinct neural substrates. *Soc Cogn*

Affect Neurosci. 2015 Apr;10(4):605-11. doi: 10.1093/scan/nsu091. Epub 2014 Jul 1. PMID: 24984958; PMCID: PMC4381244.

26. Ben-Shachar M, Lüdtke D, Makowski D (2020). effectsize: Estimation of Effect Size Indices and Standardized Parameters. *Journal of Open Source Software*, 5(56), 2815. doi: 10.21105/joss.02815

27. Xia M, Wang J, He Y (2013) BrainNet Viewer: A Network Visualization Tool for Human Brain Connectomics. PLoS ONE 8: e68910.

28. Krebs, E.E., Lorenz, K.A., Blair, M.J., et al. (2009). Development and initial validation of the PEG, a three-item scale assessing pain intensity and interference. *Journal of General Internal Medicine*, 24: 733-738.

29. Strigo IA, Matthews SC, Simmons AN, Oberndorfer T, Klabunde M, Reinhardt LE, Kaye WH. Altered insula activation during pain anticipation in individuals recovered from anorexia nervosa: evidence of interoceptive dysregulation. *Int J Eat Disord*. 2013 Jan;46(1):23-33. doi: 10.1002/eat.22045. Epub 2012 Jul 27. PMID: 22836447; PMCID: PMC3507323.

30. Craig AD. How do you feel? Interoception: the sense of the physiological condition of the body. *Nat Rev Neurosci*. 2002 Aug;3(8):655-66. doi: 10.1038/nrn894. PMID: 12154366.

31. Craig AD. Interoception and emotion: A neuroanatomical perspective. In Lewis M, Haviland-Jones JM, Barrett LF, editors. *Handbook of Emotions*, 3rd ed. New York: Guilford Publications, 2008. pp.272–288.

32. Strigo, I., Spadoni, A., Lohr, J. *et al.* Too hard to control: compromised pain anticipation and modulation in mild traumatic brain injury. *Transl Psychiatry* 4, e340 (2014). <https://doi.org/10.1038/tp.2013.116>

33. Strigo, Irina A. et al. "Repeated Exposure to Experimental Pain Differentiates Combat Traumatic Brain Injury with and Without Post-Traumatic Stress Disorder." *Journal of neurotrauma* 35.2 (2018): 297–307. Web.

35. Lee, Su-In, et al. "Efficient l_1 regularized logistic regression." *Aaai*. Vol. 6. 2006.
36. Efron, Bradley. *The jackknife, the bootstrap and other resampling plans*. Society for industrial and applied mathematics, 1982.
37. <http://wavedatalab.github.io/machinelearningwithr/post4.html#:~:text=Hence%2C%20much%20like%20the%20best,zero%20can%20be%20thrown%20away>.
38. Friedman J, Hastie T, Tibshirani R (2010). "Regularization Paths for Generalized Linear Models via Coordinate Descent." *Journal of Statistical Software*, **33**(1), 1–22. [doi:10.18637/jss.v033.i01](https://doi.org/10.18637/jss.v033.i01).
39. RStudio Team (2020). RStudio: Integrated Development for R. RStudio, PBC, Boston, MA URL <http://www.rstudio.com/>.

Publishing Agreement

It is the policy of the University to encourage open access and broad distribution of all theses, dissertations, and manuscripts. The Graduate Division will facilitate the distribution of UCSF theses, dissertations, and manuscripts to the UCSF Library for open access and distribution. UCSF will make such theses, dissertations, and manuscripts accessible to the public and will take reasonable steps to preserve these works in perpetuity.

I hereby grant the non-exclusive, perpetual right to The Regents of the University of California to reproduce, publicly display, distribute, preserve, and publish copies of my thesis, dissertation, or manuscript in any form or media, now existing or later derived, including access online for teaching, research, and public service purposes.

DocuSigned by:

Niaixin Zhang

4E53FEE628F5425...

Author Signature

12/15/2022

Date